Received: 8 August 2018 | Accepted: 25 September 2018

DOI: 10.1002/ccr3.1868

CASE REPORT

WILEY Clinical Case Reports Open Access

Novel metabolic signatures of compound heterozygous *Szt2* variants in a case of early-onset of epileptic encephalopathy

Martine Uittenbogaard[1] | **Andrea Gropman**[2] | **Christine A. Brantner**[3] | **Anne Chiaramello**[1]

[1]Department of Anatomy and Regenerative Biology, George Washington University School of Medicine and Health Sciences, Washington, District of Columbia

[2]Division of Neurogenetics and Developmental Pediatrics, Children's National Medical Center, Washington, District of Columbia

[3]GW Nanofabrication and Imaging Center, Office of the Vice President for Research, George Washington University, Washington, District of Columbia

Correspondence
Anne Chiaramello, Department of Anatomy and Regenerative Biology, George Washington University School of Medicine and Health Sciences, Washington, DC.
Email: achiaram@gwu.edu

Funding information
NIH National Institute of Neurological Disorders and Stroke [NS085282 to AC] and National Institute of Child Health and Development [1U54HD090257]

Key Clinical Message

Our study reports the case of a patient with early onset of epileptic encephalopathy harboring compound heterozygous *Szt2* variants. We provide the first evidence that these *Szt2* variants impair mitochondrial energy metabolism. Our results shed light on their pathogenic molecular mechanism and clinical implications for brain development and disease progression.

KEYWORDS

compound heterozygous mutations, energy metabolism, epileptic encephalopathy, seizure threshold 2 gene, whole-exome sequencing

1 | INTRODUCTION

In 2009, the murine seizure threshold 2 (*Szt2*) gene was discovered by a ethylnitrosourea mutagenesis screen.[1] Most notably, the Szt2 homozygous mouse mutants are prone to induced seizures. Szt2 is highly expressed in the developing and mature brain, more specifically in the parietal and frontal cortex, as well as in the dorsal root ganglia.[1] It plays a key role in brain development. The SZT2 protein is highly conserved in evolution with unknown functions until recently. The SZT2 protein is one of the components of the protein complex KICSTOR, which is composed of three additional members: KPTN, ITF2, and C12orf66.[2] SZT2 recruits GATOR1 to transiently translocate the mechanistic target of rapamycin complex I (mTORC1) to the lysosome, an important step in the nutrient-sensing mTORC1 pathway.[3] Moreover, Szt2 deficiency results in constitutive localization of mTORC1. In mice, mTORC1 signaling plays a crucial role during the transition from placental nutrition to neonatal fasting immediately after birth, when levels of amino acids and glucose concentration are down.[4]

The human *Szt2* gene (previously known as *C1orf84* and *KIAA0467*) contains 71 exons and is located on chromosome 1 p34.2. A handful of pathogenic variants has been discovered by whole-exome sequencing (WES) in pediatric

patients showing phenotypic developmental diversity with or without seizures. The initial clinical case describes biallelic pathogenic *Szt2* variants resulting in premature stop codon or exon skipping and ensuing the loss of the functional SZT2 protein in children with early-onset epileptic encephalopathy with severe intellectual disability (ID), a short and thick corpus callosum, and persistent cavum septum pellucidum.[5] A subsequent clinical case reports a homozygous three-base-pair-deletion in the *Szt2* gene of three children with nonsyndromic mild ID without seizures causing an amino acid deletion in a conserved region of the SZT2 protein.[6] Compound heterozygous frameshift and nonsense *Szt2* variants were detected in a young child presenting a different phenotype characterized by developmental delay, cognitive deficiencies, and most importantly abnormal perisylvian gyral configuration suggestive of abnormal cortical development due to abnormal neuronal migration.[7] Since then, additional novel pathogenic *Szt2* variants have been identified by WES in related and unrelated patients exhibiting a range of phenotypes.[8,9]

In this study, we report the case of a young patient harboring compound heterozygous *Szt2* variants, the maternally inherited substitution variant of uncertain significance mapping in exon 36 and the paternally inherited in-frame three-base-pair-deletion variant, likely pathogenic, mapping in exon 42. The proband exhibits severe global developmental delay, hypotonia, cognitive deficiencies, and transient seizures following a hypoxic-ischemic event closely after birth. We provide the first evidence of impaired metabolic signature of these two *Szt2* variants. We show that these compound heterozygous *Szt2* variants significantly mitigate mitochondrial energy metabolism and glycolysis by curtailing the mitochondrial spare respiratory capacity and compensatory glycolytic response, respectively. Taken together, our collective findings reveal a dysregulated metabolic reprogramming that prevents an efficient switch from OXPHOS to glycolysis resulting in an exacerbated energy crisis with implications for brain development and disease progression.

2 | MATERIALS AND METHODS

2.1 | Editorial policies and ethical considerations

This study was approved by the Institutional Review Board of the George Washington University and Children's National Medical Center and was conducted in accordance with the ethical principles of the Declaration of Helsinki of 1975 (revised 1983). Patient skin biopsy was performed only after receiving written informed consent with permission to study the derived dermal fibroblasts.

2.2 | Skin biopsy and fibroblast culture

Skin biopsy was performed on a 4-year-old proband. Dermal fibroblasts were derived from 3-mm skin biopsy in Dulbecco's modified Eagle medium (DMEM; Gibco Laboratories, Gaithersburg, MD, USA) supplemented with 2 mmol/L glutamine, 2.5 mmol/L pyruvate, 0.2 mmol/L uridine, FGF-2 (10 ng/mL), and 20% fetal bovine serum, as described in.[10] Derived dermal fibroblasts were frozen at passage 2 and never used beyond passage 10. Human primary dermal fibroblasts from a healthy child (Cat# GM03349C) were obtained from the Coriell Cell Repositories (Camden, NJ).

2.3 | Clinical genetic diagnosis

Whole-exome sequencing (WES) and next-generation sequencing (NGS) of the mitochondrial genome were performed by GeneDx using dermal fibroblasts from the proband.

2.4 | Transmission electron microscopy

Dermal fibroblasts from the proband and the control (healthy child) were fixed in 2.5% glutaraldehyde (Electron Microscopy Sciences), 1% paraformaldehyde in 0.12 mol/L sodium cacodylate buffer (Electron Microscopy Sciences) for 20 minutes at room temperature followed by 40 minutes on ice, as described in.[10] Briefly, cells were then fixed for one hour in 1% osmium tetroxide (Electron Microscopy Sciences) followed by *en bloc* staining overnight in 1% aqueous uranyl acetate. The cells were then dehydrated through a series of ethyl alcohol/deionized water solutions and propylene oxide before infiltration with Embed 812 epoxy resin. Blocks were cured for 48 hours at 60°C. Polymerized blocks were trimmed, and 70-nm-ultrathin sections were cut with a diamond knife on a Leica Ultramicut EM UC7 and transferred onto 200 mesh copper grids. Sections were counterstained with 1% ethanolic uranyl acetate for 10 min and lead citrate for 2 minutes. Samples were imaged with a FEI Talos F200X transmission electron microscope (FEI Company) operating at an accelerating voltage of 80 kV equipped with a Ceta™ 16M camera.

2.5 | Analysis of mitochondrial respiration and glycolysis

Bioenergetic status was measured using the Seahorse Extracellular Flux XFp Analyzer (Seahorse Bioscience, Agilent Technologies). Optimal cell density (5000/well) and the uncoupler FCCP (fluoro 3-carbonyl cyanide-methoxyphenyl hydrazine; 2 μmol/L) were determined using the Cell Energy Phenotype Test kit. Skin fibroblasts were seeded in triplicate on poly-D lysine-coated plates and incubated for 24 hours at 37°C in 5% CO2 atmosphere. Prior to the assay, the supplemented DMEM medium was changed

to unbuffered base medium supplemented with 2 mmol/L glutamine (Invitrogen), 2 mmol/L pyruvate (Sigma), and/or 7.1 mmol/L glucose (Sigma) depending on the assay and adjusted to at pH 7.4 with NaOH for one hour at 37°C. Using the XFp Mito Stress Test kit, OCR (oxygen consumption rate) and ECAR (extracellular acidification rate) were measured under basal conditions and after sequential injections of oligomycin (1 µmol/L), FCCP (2 µmol/L), and a mix of rotenone and antimycin A (1 µmol/L) following manufacturer's recommendations. Using the XFp Glycolysis Stress Test kit, we measured the glycolytic functions under initial glucose starvation and subsequent sequential injections of saturated glucose concentration (10 mmol/L), oligomycin (1 µmol/L), and 2-DG (50 mmol/L). Using the Glycolytic Rate Assay kit, we determined the total proton efflux and the glycolytic proton efflux by measuring the OCR and ECAR values. Prior to the assay, the supplemented DMEM medium was changed to the XF Base medium without phenol red supplemented with 2 mmol/L glutamine, 10 mmol/L glucose, 1 mmol/L pyruvate, and 5.0 mmol/L HEPES. OCR and ECAR were measured under basal conditions and after sequential injections of rotenone/antimycin A (0.5 µmol/L final concentration) and 2-DG (50 mmol/L final concentration). The data were normalized to cell numbers and plotted as OCR (pmol/min/cell ± SD) and ECAR (mpH/min/cell ± SD) as a function of time using the Seahorse Report Generator software. Statistical analyses were performed using the unpaired student *t* test with *P* value of less than 0.05 considered statistically significant.

3 | RESULTS

3.1 | Clinical history

The proband is a 4-year-old boy with history of global developmental delay, including significant delay in the adaptive and communication skills, profoundly abnormal oral and motor functions with visual apraxia, and global hypotonia essentially causing significant motor delay. He is nondysmorphic with normal sclera and lashes and ears normally positioned. His digits, nails, and palmar creases are normal. There are no neurocutaneous markings. His thyroid is not enlarged. Abdomen examination did not reveal hepatosplenomegaly. There are no cardiovascular problems. He wears glasses for his myopia. The proband has a 2-year-old sister, who is asymptomatic.

The mother had a normal first pregnancy with no complications and no medication exposure. This proband's parents are nonconsanguineous. He was born full-term via normal vaginal delivery. He cried quickly after birth with normal Apgar scores of 8 and 9 at 1 and 5 minutes, respectively. After one hour of life, the mother found him apneic and in cardiac arrest while breastfeeding although it was not clear whether the proband was successfully breastfed. CPR was started and heart rate recovered. He was intubated for about one hour and then extubated. In addition, the proband also had shaking movements that were thought to be seizures and was treated with phenobarbital. After the event at birth, the proband had lactate levels at 5.6 mg/mL, which were corroborated by 1H magnetic resonance spectroscopy (MRS). They subsequently decreased between 2.3 and 3.4 mg/mL. On day of life (DOL) 1, a brain computed tomography (CT) scan was performed, which showed increased signal bilaterally in the putamen. At 6 days of age, an electroencephalogram (EEG) was performed and indicated excessive left and right frontal sharp wave discharges, but no seizures. At 2 weeks of age, a brain magnetic resonance imaging (MRI) was performed, which revealed increased T2 signal in the basal ganglia with possible involvement of the globus pallidum, consistent with a neonatal hypoxic-ischemic injury (Figure 1). Due to persistent difficulty swallowing, the proband required a gastronomy tube.

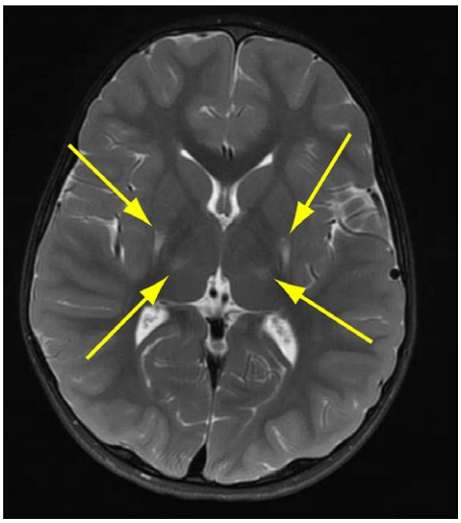

FIGURE 1 Brain magnetic resonance imaging of the proband. The panel illustrates the T2-weighted image showing gliotic changes in the bilateral putamen and posteriorly and anterolateral thalami (arrows)

Since birth, his development was delayed. He sat when he was about 1 year old and never walked. Language is only babbling with no words. He can smile, laugh, and cry. However, he cannot effectively communicate and occasionally indicates what he wants by looking at an object. With physical therapy, he was slightly improving in terms of movements by taking some steps with his gait trainer.

At the age of three, he stopped taking phenobarbital and keppra for seizures since three consecutive EEGs showed the absence of seizures. However, his encephalopathy, which used to be static, has worsened since he has regressed despite receiving physical therapy at home. He had instances in which he was not interactive with his family. In addition, he has experienced difficulty sleeping, sleeping only 3-4 hours a night. He has become much more irritable and cries a lot. He has suffered from reflux and has been on ranitidine. He has

recently experienced a severe constipation with one bowel movement every 3 weeks and started on lactulose. He remains G-tube fed with an 800 cc of EleCare (27 kcal/lf oz) per day, which is below his goal. His feeding intolerance is mainly due to his reflux and resulted in no weight gain for the last 2 years, which might be in part responsible for his failure to thrive. He has been hospitalized twice for pneumonia. Cranial nerve examination revealed low tone of the facial nerve resulting in increased drooling and a uvula—oral motor gag consistent with decreased oral motor tone.

At the age of four, the proband was genetically tested for whole-exome sequencing (WES) and next-generation sequencing of the mitochondrial genome. While no mutations, deletions, and duplications were detected in his mitochondrial genome, WES detected compound heterozygous recessive mutations mapping in the *Szt2* (seizure threshold 2) gene linked to epileptic encephalopathy early infantile 18 (OMIM 615463). The c.5174 C>T (p.A1725V) variant is maternally inherited, while the c.5949_5951del TGT (p.V1984del) variant is paternally inherited. Both were submitted to ClinVar (https://www.ncbi.nlm.nih.gov/clinvar) and have the accession number, SCV000572645.3 or SCV000491431.1, for the c.5174 C>T variant or c.5949_5951delTGT variant, respectively. The c.5174 C>T variant, which has been not been reported as pathogenic or benign, causes a conserved amino acid substitution in a nonconserved position of the SZT2 protein and is speculated to unlikely impact the secondary structure of the SZT2 protein. The rare c.5949_5951delTGT variant causes deletion of a valine residue at position 1984 in the SZT2 protein (p.Val1984del) and is characterized as likely pathogenic. Finally, the proband also carries the paternal recessive mutation c.818 C>T (p.T273M), which is a variant of uncertain significance mapping in the *Alpl* (alkaline phosphatase liver/bone/kidney) gene. It is associated with infantile hypophosphatasia (OMIM 171760). All three variants are located on the short arm of chromosome 1, with the *Szt2* and *Alpl* genes mapping on p34.2 and p.36.2, respectively. Sequencing of the proband's mitochondrial genome failed to reveal any mutation, deletion, or duplication.

3.2 | Functional outcome of the compound heterozygous Szt2 variants on mitochondrial respiration activities

Since the SZT2 protein is a component of the KICSTOR complex involved in modulating the activity of the mechanistic target of rapamycin complex I (mTORC1) known to regulate mitochondrial respiration,[2] we investigated whether the compound heterozygous *Szt2* variants could alter the mitochondrial energy metabolism in the proband's fibroblasts. As a control, we used dermal fibroblasts derived from a healthy child. Using the Seahorse Extracellular Flux XFp Analyzer, we performed live-cell respiration assays to measure the oxygen consumption rate (OCR), a key functional indicator of the mitochondrial oxidative phosphorylation (OXPHOS) pathway. We initially determined

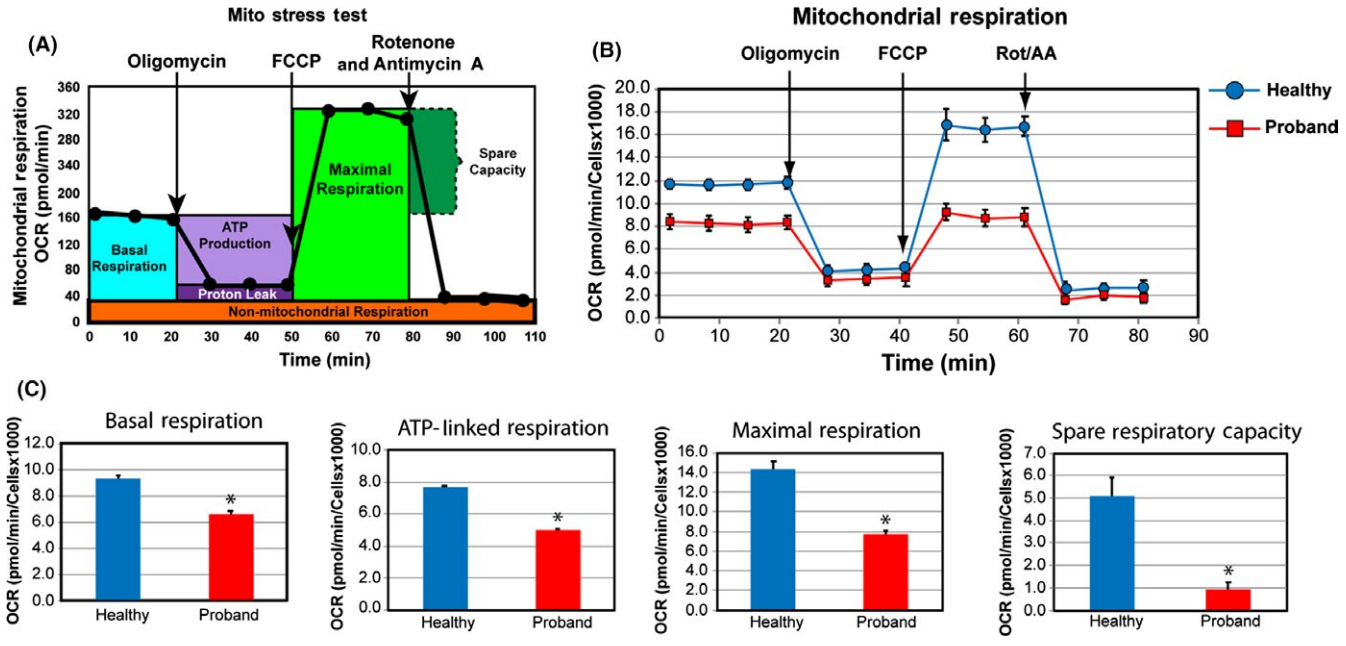

FIGURE 2 Impaired mitochondrial respiratory functions in the proband's fibroblasts. A, Profile of the oxygen consumption rate (OCR) adapted from Agilent Technologies brochure of the Mitochondrial Stress Test. B, Compared OCR responses between the proband and a healthy subject. C, Quantitative data between the proband and the healthy subject of basal respiration, ATP-linked respiration, maximal respiration, and spare respiratory capacity. Data are represented as means ± SD, n = 3 of three independent experiments. * indicates statistically significant differences with a *P* value of ≤0.0001 between the proband and the healthy subject

the optimal cell seeding density (5000 cells/well) and the concentration of the uncoupler FCCP (2 μmol/L). We next measured several key mitochondrial bioenergetics parameters of the OXPHOS pathway (Figure 2A,B). We detected a 29% decrease in the basal respiration rate of the proband's fibroblasts when compared to that of a healthy child, indicative of reduced substrate oxidation and ATP turnover (Figure 2C). Similarly, exposure to oligomycin, an inhibitor of the ATP synthase, revealed a 35% decrease in ATP-linked respiration (Figure 2C). Upon exposure to FCCP, these compound recessive *Szt2* variants significantly decreased the maximal respiration capacity by 48%, while nearly abolishing the spare respiratory capacity to 19% residual levels, indicative of a severely stunted ability to surmount a bioenergetic crisis (Figure 2C). Collectively, our bioenergetics results provide the first evidence that these compound heterozygous *Szt2* variants significantly repress the overall OXPHOS activities.

3.3 | Mitochondrial morphometric analysis of the dermal fibroblasts derived from the proband

By transmission electron microscopy, we investigated whether mitochondria from the proband's fibroblasts exhibited ultrastructural defects. As expected, fibroblasts from a healthy child harbored long mitochondria with a normal morphology characterized with numerous cristae and electron-dense mitochondrial matrix (Figure 3A). The proband's fibroblasts contain few mitochondria with a normal morphology and well-developed cristae and a preponderance of mitochondria with abnormal cristae morphology (Figure 3B). Of note, some mitochondria had an exaggerated elongated morphology, suggestive of dysregulated mitochondrial dynamics (Figure 3B). In addition, the proband's fibroblasts have endoplasmic reticulum (ER) with enlarged saccules, characteristic of ER stress, along with an abundance of lysosomes filled with undigested membranes indicative of autophagy. Thus, our mitochondrial morphometric findings concord with declined mitochondrial respiratory activities in the presence of these compound heterozygous *Szt2* variants.

3.4 | Functional outcome of the compound heterozygous Szt2 variants on glycolytic activities

Given the sharply reduced OXPHOS activities, we investigated whether the proband's fibroblasts could meet the energy demand via glycolysis. To address this question, we used two distinct, but complementary, assays to interrogate

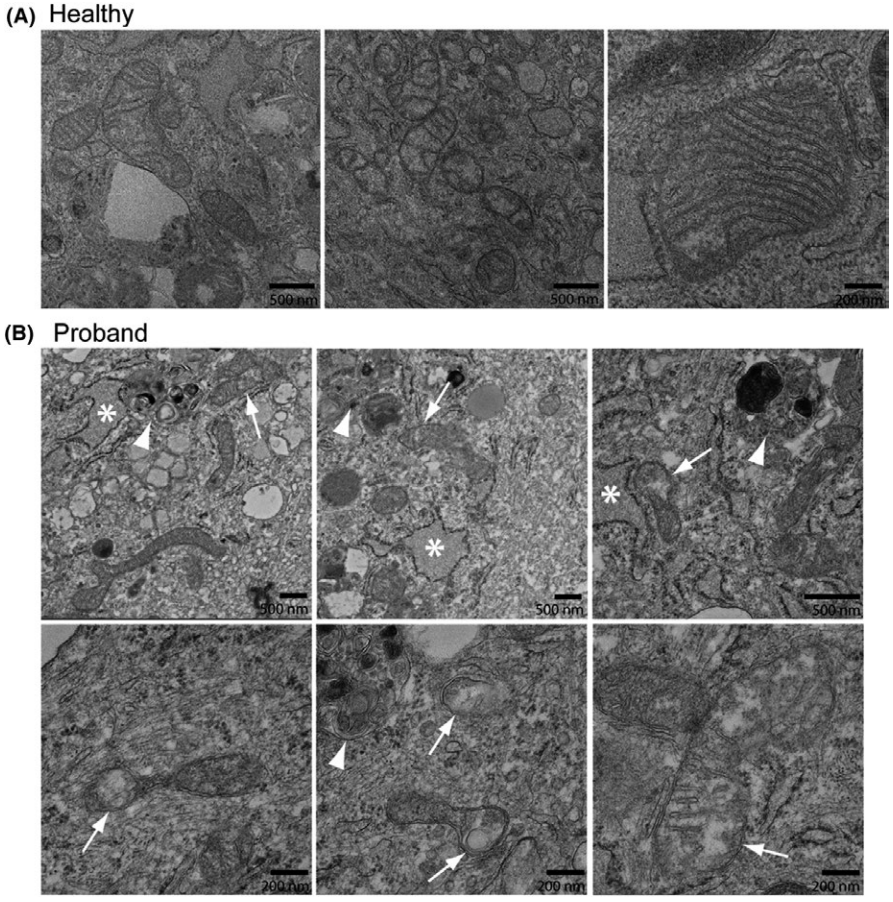

FIGURE 3 The compound heterozygous *Szt2* variants, c.5174 C>T (p.A1725V) and c.5949_5951del TGT (p.V1984del), alter the morphology of cristae and cause excessive mitochondrial elongation. A, Mitochondrial morphometric analysis by transmission electron microscopy using dermal fibroblasts from a healthy subject. The scale bar is indicated at the bottom right corner of each micrograph. B, Mitochondrial morphometric analysis by transmission electron microscopy using dermal fibroblasts from the proband. The scale bar is indicated at the bottom right corner of each micrograph. The white arrows indicate mitochondrial with abnormal cristae, while the white arrowheads indicate abundant lysosomes containing undigested membranes. The white asterisk denotes endoplasmic reticulum with enlarged saccules

glycolysis using different parameters and conditions. The Glycolysis Stress Test assesses glycolysis by quantifying changes in pH (ECAR) after having starved the fibroblasts for glucose followed by injection of saturating concentration of glucose (10 mmol/L) that fuels both glycolysis and mitochondrial OXPHOS, followed by an injection of oligomycin to inhibit mitochondrial ATP synthase, and a final injection of 2-deoxyglucose to inhibit glucose catabolism (Figure 4A). In the presence of saturated glucose concentration, the slight decrease in glycolysis between the proband's fibroblasts and control healthy fibroblasts was not statistically significant (Figure 4B,C). Upon inhibition of respiratory ATP production, the maximum glycolytic capacity of the proband's fibroblasts declined by 21% when compared to that of a healthy child (Figure 4B,C), revealing that the proband's fibroblasts could not sufficiently augment glycolysis to compensate for the loss of mitochondrial ATP production. Finally, inhibition of the glucose metabolism by 2-DG reduced the glycolytic reserve by 35% in the proband's fibroblasts, when compared to that of a healthy subject (Figure 4B,C).

Since quantifying glycolysis using the Glycolysis Stress Test assay overestimates the true basal glycolysis, we supplemented our analysis with the Glycolysis Rate Test assay. While ECAR values derived from the Glycolysis Stress Test assay measure bulk acidification as a result of protons from the conversion of pyruvate to lactate and from the mitochondrial CO_2 production as a by-product of the TCA cycle resulting in acidification from the produced six protons per molecule of glucose,[13] the glycolytic proton efflux rate (GlycoPER) correlates one-to-one with lactate accumulation as a result of glycolysis. Thus, we measured the total proton efflux rate (PER) and GlycoPER to evaluate the functional impact of these two *Szt2* variants on glycolysis under physiological conditions (ie, the absence of glucose starvation). The proband's fibroblasts displayed a 35% decrease in basal glycolysis when compared to that of the healthy fibroblasts, indicative of a substantial decrease in the proband's authentic ability for basal glycolysis (Figure 5C). We assessed the compensatory glycolysis response upon complete inhibition of mitochondrial OXPHOS by blocking the activity of the respiratory complexes I and III via rotenone and antimycin A, respectively.[14] The proband's fibroblasts showed a substantial decrease in compensatory glycolysis by 35%, when compared to that of healthy fibroblasts (Figure 5C). This response is consistent with the reduced glycolytic reserve quantified using the glycolysis stress test assay (Figure 4C), indicating that the proband's fibroblasts exhibit a diminished glycolysis response when mitochondrial respiration is blocked either at the complexes I and III or complex V (ATP synthase). Finally, we found that the proband's fibroblasts exhibited a 19% decrease in mitochondrial acidification than healthy fibroblasts (Figure 5B,C), in keeping with the decreased mitochondrial OXPHOS metabolism (Figure 2).

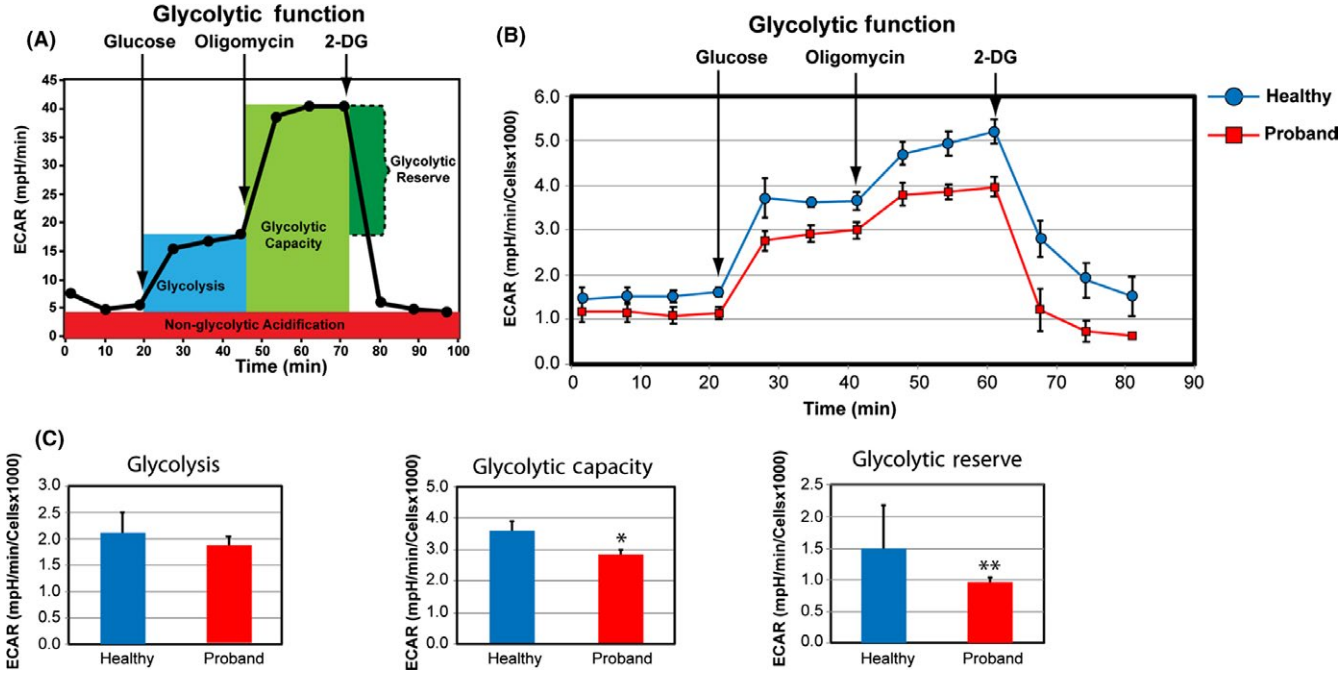

FIGURE 4 Impaired glycolytic activity in the proband's fibroblasts. A, Profile of the extracellular acidification rate (ECAR) adapted from the Agilent Technologies brochure of the Glycolysis Stress Test. B, Compared ECAR responses between the proband and a healthy subject. C, Quantitative data of glycolysis, glycolytic capacity, and glycolytic reserve. Data are represented as means ± SD, n = 3 of three independent experiments. * and ** indicate statistically significant differences with a *P* value of 0.037 and 0.006 between the proband and the healthy subject

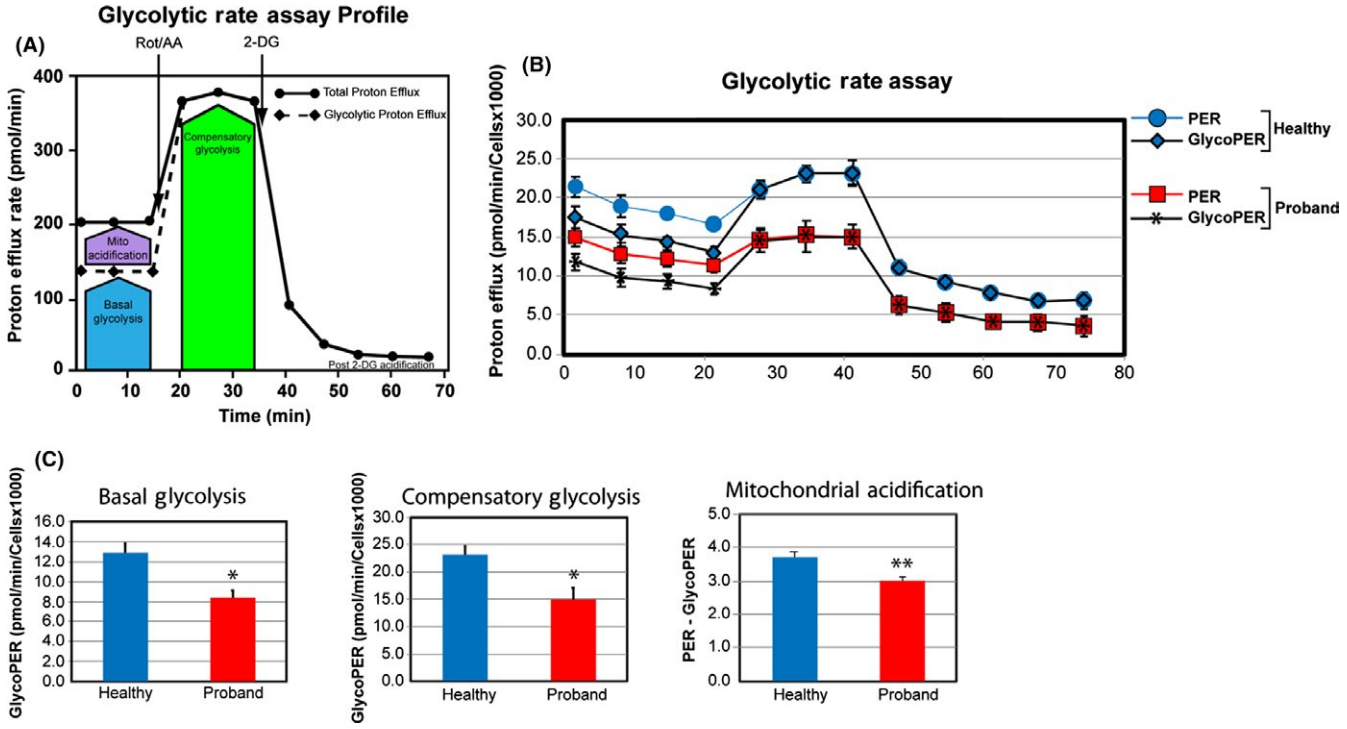

FIGURE 5 Altered glycolytic adaptation in the proband's fibroblasts. A, Schematic representation of proton efflux adapted from the Agilent Technologies brochure of the Glycolytic Rate Test. B, Compared proton efflux rate between the proband and healthy subject. C, Quantitative data of basal glycolysis, compensatory glycolysis, and mitochondrial acidification. Data are represented as means ± SD, n = 3 of three independent experiments. * and ** indicate statistically significant differences with a *P* value of ≤0.005 and 0.04 between the proband and the healthy subject

4 | DISCUSSION

Our study reports a patient harboring compound heterozygous *Szt2* variants, the maternally inherited c.5174 C>T (p.A1725V) and the paternally inherited c.5949_5951del TGT (p.V1984del), which have not been previously communicated. Furthermore, we provide novel evidence of metabolic and mitochondrial dysfunctions by these compound heterozygous *Szt2* variants, shedding light on the potential pathophysiologic mechanism and genotype-phenotype correlations. Since 2013, up to 15 *Szt2* variants have been identified in patients with early-onset epileptic encephalopathy.[5–7] Although these patients exhibit heterogeneous clinical phenotypes, they all show developmental delay to various degrees with or without epilepsy, most likely correlated to the residual functions of the SZT2 protein. Biallelic truncating mutations cause the most extreme phenotypic manifestations, such as severe developmental delay, profound intellectual disability, the absence of speech, facial dysmorphism, focal epileptic discharges, pectus carinatum, and a thick and short corpus callosum.[5,7] In contrast, missense *Szt2* variants are associated with mild phenotype including moderate intellectual disability without seizures, most likely as a result of residual SZT2 functions.[6]

Although our proband harbors a maternally inherited missense *Szt2* variant and a paternally inherited in-frame deletion *Szt2* variant, he exhibits a clinical phenotype overlapping with that of patients harboring biallelic truncating mutations. He presents severe developmental delay, the absence of speech, global hypotonia, cognitive deficiencies, and transient seizures following a hypoxic-ischemic event closely after birth. However, he exhibits persistent swallowing problems and severe intestinal problems not previously reported in patients harboring other *Szt2* variants. His clinical symptoms were not due to mutation(s) in the mitochondrial genome, as his NGS results came back negative for variants, indicating that the *Szt2* variants detected by WES were causing his clinical phenotype. The proband's *Szt2* missense and in-frame deletion variants map in exon 36 and exon 42 of the *Szt2* gene, two genomic locations not been previously documented in other patients. At the protein level, both variants map within a domain rich in alpha-helices, as revealed by protein modeling using ModBase.[15] Most notably, the maternal variant maps within the GATOR1-binding region (amino acids 935-1734), relevant to the recently discovered Szt2 function.[3]

SZT2, along with three other components of the KICSTOR complex (KPTN, ITFG2 and C12orf66), is essential of the KICSTOR complex, is essential for forming a SZT2-orchestrated GATOR (SOG) complex that controls recruitment of the master growth regulator mechanistic target of rapamycin complex I (mTORC1) complex to lysosomes.[3] SZT2 represses mTORC1 activation in part by binding and

tethering GATOR1 to the lysosomal membranes to inhibit RAG GTPase proteins,[2] a process that is regulated by amino acid-sensing mechanisms.[16] Amino acid sufficiency inhibits GATOR1, thereby allowing active Rag heterodimer to interact and recruit mTORC1 complex to the lysosomal membranes for mTORC1 activation, which prevents autophagy. In contrast, amino acid-deficient conditions prevent mTORC1 recruitment to lysosomal membranes due to GATOR1-mediated inhibition of RAG GTPase proteins, thereby inhibiting mTORC1 activation and allowing autophagy. Since the integrity of SOG is pivotal for its localization at the lysosomes, Szt2 deficiency results in constitutive mTORC1 localization at the lysosome irrespective of nutrient status.[3] mTORC1 hyperactivation being frequently associated with epilepsy is congruent with enhanced neuronal mTORC1 signaling in Szt2-/- mice.[17,18] Furthermore, the postnatal lethality of Szt2-/- mice due to fasting at weaning age is consistent with the reported impaired early postnatal survival in mice expressing a constitutively active form of RagA.[3] Rag-mediated regulation of mTORC1 is necessary for neonates to survive the starvation period triggered by interruption of maternal nutrient supply at birth. Between birth and suckling, mTORC1 inhibition triggers autophagy to generate gluconeogenic amino acids in order to sustain plasma glucose levels. Thus, it is highly plausible that *Szt2* deficiency prevents autophagy due to constitutive mTORC1 activation, resulting in dysregulated neonatal nutrient sensing and subsequent glucose starvation. The deficient neonatal nutrient switch mediated by these compound heterozygous *Szt2* variants may have in part caused neonatal hypoxic-ischemia in the proband during his initial breastfeeding.

Our live-cell metabolic study provides the first evidence of dysregulated mitochondrial energy metabolism in a patient harboring *Szt2* variants. The maternally inherited c.5174 C>T (p.A1725V) and the paternally inherited c.5949_5951del TGT (p.V1984del) *Szt*2 variants reduce the overall metabolic activity of the mitochondrial oxidative phosphorylation (OXPHOS) pathway in the proband's fibroblasts with a decline in basal respiration and ATP-linked respiration resulting from decreased substrate oxidation. Most notably is the near abolishment of the spare respiratory capacity to 19% of residual levels, which severely stunts the ability to assume a sudden increase in energy demand, thereby crippling cell survival.[19] The metabolic disturbance caused by these two *Szt2* variants is relevant to the neurological manifestations of the proband, such as developmental delay, intellectual disability, seizures, and global hypotonia. Neuronal differentiation and proper temporal and spatial neuronal migration during neurogenesis are highly dependent on mitochondrial biogenesis and bioenergetics.[20] Our live-cell bioenergetic findings support previous studies demonstrating the role of mTORC1 in energy metabolism by bolstering mitochondrial ATP levels via the OXPHOS pathway and mitochondrial biogenesis.[11,21–23] Mitochondrial dysfunction caused by these two *Szt*2 variants is not limited to bioenergetics based on the excessive mitochondrial elongation phenotype in the proband's fibroblasts, suggestive of dysregulated mitochondrial dynamics. This is consistent with recent studies showing that mTORC1 stimulates mitochondrial fission via 4E-BP-mediated translational regulation of the mitochondrial fission factor MTFP1 and conversely mTOR inhibition leads to mitochondrial hyperfusion.[24]

Finally, our studies provide a novel metabolic perspective of these two *Szt2* variants by highlighting decreased glycolytic activities with a lessened glycolytic reserve. More specifically, the proband's fibroblasts show a reduced basal glycolysis and compensatory glycolysis. Taken together, these bioenergetic findings demonstrate that these compound heterozygous *Szt2* variants dysregulate energy reprogramming as a result of a curtailed ability to switch to glycolysis upon full inhibition of mitochondrial OXPHOS. Therefore, these *Szt2* variants prevent an effective interplay between the two main energy pathways, OXPHOS and glycolysis, which is critical to sustain ATP synthesis under conditions simulating an acute energy crisis. A similar defective metabolic switch was detected in the presence of the m.8993T>G variant mapping in the mitochondrial *MT-ATP6* gene encoding the subunit 6 of the ATP synthase associated with the maternally inherited form of Leigh syndrome.[10] Our metabolic findings are consistent with the previously reported link between mTORC1 activation and genes encoding the enzymes of glycolysis.[21]

In conclusion, our collective findings on mitochondrial morphometry and metabolic studies provide important and novel insights into the contributions of mTORC1 to the metabolic reprogramming in response to pathological activation by two *Szt2* variants. In addition, our results highlight a potential pathomechanism underlying the onset and development of early epileptic encephalopathy in a patient harboring compound heterozygous *Szt2* variants.

ACKNOWLEDGMENTS

We thank Meira Meltzer for her help with the genetic testing results and for coordinating patient care with the skin biopsy.

CONFLICT OF INTEREST

The authors have no conflict of interests to declare.

AUTHOR CONTRIBUTION

MU and AC: designed the experimental approaches. CAB: planned and performed the experiments related to transmission electron microscopy and processed all the images for

analysis. AG: performed the skin biopsy on the patient under her care and provided the corresponding clinical assessment and interpretation of the neurological and biological tests. MU: conducted all the bioenergetic assays. AC: wrote the manuscript.

ORCID

Anne Chiaramello http://orcid.org/0000-0001-8424-0826

REFERENCES

1. Frankel WN, Yang Y, Mahaffey CL, Beyer BJ, O'Brien TP. *Szt2*, a novel gene for seizure threshold in mice. *Genes Brain Behav*. 2009;8:568-576. https://doi.org/10.1111/j.1601-183X.2009.00509.x.
2. Wolfson RL, Chantranupong L, Wyant GA, et al. KICSTOR recruits GATOR1 to the lysosome and is necessary for nutrients to regulate mTORC1. *Nature*. 2017;543:438-445. https://doi.org/10.1038/nature21423.
3. Peng M, Yin N, Li MO. SZT2 dictates GATOR control of mTORC signaling. *Nature*. 2017;543:433-437. https://doi.org/10.1038/nature21378.
4. Efeyan A, Zoncu R, Chang S, et al. Regulation of mTORC1 by the Rag GTPases is necessary for neonatal autophagy and survival. *Nature*. 2013;493:679-684. https://doi.org/10.1038/nature11745.
5. Basel-Vanagaite L, Herhkovitz T, Heyma E, et al. Biallelic SZT2 mutations cause infantile encephalopathy with epilepsy and dysmorphic corpus callosum. *Am J Human Genet*. 2013;93:524-529. https://doi.org/10.1016/j.ajhg.2013.07.005.
6. Falcone M, Yariz KO, Ross DB, Foster J II, Menendez I, Tekin M. An amino acid deletion in SZT2 in a family with non-syndromic intellectual disability. *PLoS ONE*. 2013;8(12):e82810. https://doi.org/10.1371/journal.pone.0082810.
7. Venkatesan C, Angle B, Millichap JJ. Early-life epileptic encephalopathy secondary to *SZT2* pathogenic recessive variants. *Epileptic Dis*. 2016;18:195-200. https://doi.org/10.1684/epd.2016.0828.
8. Nakamura Y, Togawa Y, Okuno Y, et al. Biallelic mutations in SZT2 cause a discernible clinical entity with epilepsy, developmental delay, macrocephaly and a dysmorphic corpus callosum. *Brain Develop*. 2018;40:134-139. https://doi.org/10.1016/j.braindev.2017.08.003.
9. Tsuchida N, Nakashima M, Miyauchi A, et al. Novel biallelic SZT2 mutations in 3 cases of early-onset epileptic encephalopathy. *Clin Genet*. 2018;93:266-274. https://doi.org/10.1111/cge.13061
10. Uittenbogaard M, Brantner CA, Fang S, Wong J-C, Gropman A, Chiaramello A. Novel insights into the functional metabolic impact of an apparent de novo m.8993T>G variant in the *MT-ATP6* gene associated with maternally inherited form of Leigh syndrome. *Mol Genet Metab*. 2018;124:71-81. https://doi.org/10.1016/j.ymgme.2018.03.011.
11. Cunnigham JT, Rodgers JT, Arlow DH, Vazquez F, Mootha VK, Puigserver P. mTOR controls mitochondrial oxidative function through a YY1-PGC-1alpha transcriptional complex. *Nature*. 2007;450(7170):736-740. https://doi.org/10.1038/nature06322.
12. Ramanathan A, Schreiber SL. Direct control of mitochondrial function by mTOR. *Proc Natl Acad Sci*. 2009;106(52):22229-22232. doi/10.1073/pnas.0912074106.
13. Mookerjee SA, Goncalves RLS, Gerencser AA, Nicholls DG, Brand MD. The contributions of respiratory and glycolysis to extracellular acid production. *Biochem Biophys Acta*. 2015;1847:171-181. https://doi.org/10.3791/53464.
14. Mookerjee SA, Nicholls DG, Brand MD. Determining maximum glycolytic capacity using extracellular flux measurements. *PLoS ONE*. 2016;11(7):e0159199. https://doi.org/10.1371/journal.pone.0152016.
15. Pieper U, Webb B, Dong GQ, et al. ModBase, a database of annotated comparative protein structure models and associated resources. *Nucleic Acids Res*. 2014;42:D336-D346. https://doi.org/10.1093/nar/gkt1144.
16. Lim C-Y, Zoncu R. The lysosome as a command-and-control center for cellular metabolism. *J Cell Biol*. 2016;214(6):653-644. https://doi.org/10.1083/jcb.201607005.
17. Laplante M, Sabatini DM. mTOR signaling in growth control and disease. *Cell*. 2012;149:274-293. https://doi.org/10.1016/j.cell.2012.03.017.
18. Sadowski K, Kotulska-Jóźwiak K. Role of mTOR inhibitors in epilepsy treatment. *Pharmacol Rep*. 2015;67:636-646. https://doi.org/10.1016/j.pharep.2014.12.017.
19. Yadava N, Nicholls DG. Spare respiratory capacity rather than oxidative stress regulates glutamate excitotoxicity after partial respiratory inhibition of mitochondrial complex I with rotenone. *J Neurosci*. 2007;27:7310-7317. https://doi.org/10.1523/JNEUROCI.0212-07.2007.
20. Uittenbogaard M, Chiaramello A. Mitochondrial biogenesis: a therapeutic target for neurodevelopmental disorders and neurodegenerative diseases. *Curr Pharm Des*. 2014;20:5574-5593. https://doi.org/10.2174/1381612820666140305224906.
21. Düvel K, Yecies JL, Menon S, et al. Activation of a metabolic gene regulatory network downstream of mTOR complex 1. *Mol Cell*. 2010;39:171-183. https://doi.org/10.1016/j.molcel.2010.06.022.
22. Morita M, Gravel S-P, Chénard V, et al. mTORC1 controls mitochondrial activity and biogenesis through 4E-BP-Dependent translational regulation. *Cell Metab*. 2013;18:698-711. https://doi.org/10.1016/j.cmet.2013.10.001.
23. Schieke SM, Phillips D, McCoy JP, et al. The mammalian target of rapamycin (mTOR) pathway regulates mitochondrial oxygen consumption and oxidative capacity. *J Biol Sci*. 2006;281(37):27643-27652. https://doi.org/10.1074/jbc.M603536200.
24. Morita M, Prudent J, Basu K, et al. mTOR controls mitochondrial dynamics and cell survival via MTFP1. *Mol Cell*. 2017;67:922-935. https://doi.org/10.1016/j.molcel.2017.08.013.

How to cite this article: Uittenbogaard M, Gropman A, Brantner CA, Chiaramello A. Novel metabolic signatures of compound heterozygous *Szt2* variants in a case of early-onset of epileptic encephalopathy. *Clin Case Rep*. 2018;6:2376–2384. https://doi.org/10.1002/ccr3.1868